JOC*Article*

Carbocations $(M + H)^+$ and Oxidation Dications (M^{2+}) from Benzo[*a*]pyrene and Its Nonalternant Isomers Azulenophenalenes: A Theoretical (DFT, GIAO, NICS) Study

Takao Okazaki[†,‡] and Kenneth K. Laali[*,‡]

Department of Energy and Hydrocarbon Chemistry, Kyoto University, Kyoto, Japan, and Department of Chemistry, Kent State University, Kent, Ohio 44242

klaali@kent.edu

Received August 1, 2003

The arenium ions of protonation and the two-electron oxidation dications derived from benzo[*a*]-pyrene (BaP) **1** and three of its nonalternant isomers namely azuleno[5,6,7-*cd*]phenalene **2** (a strong carcinogen reported to be as potent as BaP) azuleno[1,2,3-*cd*]phenalene **3** (a strong mutagen/weak carcinogen), and azuleno[4,5,6-*cd*]phenalene **4** (a weak mutagen) were studied by DFT at the B3LYP/6-31G(d) level. The most favored sites for electrophilic attack were identified on the basis of relative protonation energies in the arenium ions. Computed NMR chemical shifts (GIAO NMR), the NPA-derived charges (and changes in charges), as well as NICS (and ΔNICS) were employed to derive charge delocalization maps and to gauge relative aromaticity/antiaromaticity in the resulting carbocations and oxidation dications. Quantitative correlations between the experimental (superacid) ^{13}C data and GIAO chemical shifts, and between computed changes in charges and GIAO $\Delta\delta$ ^{13}C values were explored for benzo[*a*]pyrenium ion (**1cH**$^+$) and its singlet oxidation dication (**1**$^{2+}$) as representative cases. For the studied PAHs (**1**−**4**), formation of singlet dications were computed to be strongly favored except in **4** for which the triplet lies 5 kcal/mol lower than singlet. Relative carbocation stability data and the derived charge delocalization patterns are assessed in light of the available chemical and toxicological data on these compounds. The present study is the first of its kind to examine the carbocations and oxidation dications derived from biologically active nonalternant analogues of BaP for which no stable ion data are available. It also validates and extends the experimental data for BaP carbocation and oxidation dication and provides a means to gauge the success of GIAO NMR in predicting NMR data for PAH-arenium ions.

Introduction

Benzo[*a*]pyrene (BaP) **1** (Figure 1) and its oxidized metabolites are among the most intensely investigated classes of PAHs that played a major role in the development of "bay-region theory" and in elucidation of structure/activity relationships and bioactivation mechanisms.[1−3] Benzo[*a*]pyrene continues to serve as a benchmark in DNA-binding studies and carcinogenicity measurements.[4]

In comparison to a wealth of structural/mechanistic, synthetic, and toxicological data on BaP and its oxidized metabolites, theoretical studies at sufficiently high levels focusing on BaP-derived carbocations as models of biological electrophiles are surprisingly rare.[5a] Ring opening of protonated BaP epoxide and diol-epoxide was recently

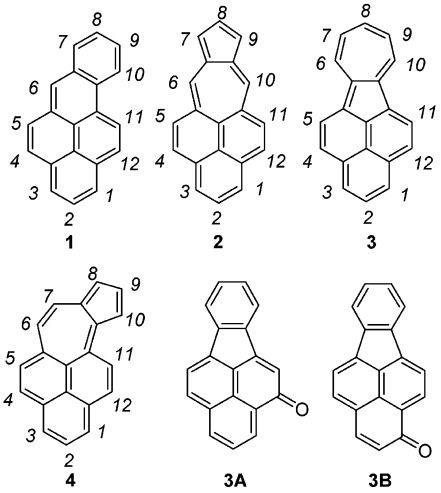

FIGURE 1. Benzo[*a*]pyrene (**1**), isomeric azulenophenalenes (**2**-**4**), 4-oxo-4*H*- benzo[*cd*]fluoranthene (**3A**), and 1-oxo-1*H*-benzo[*cd*]fluoranthene (**3B**).

* To whom correspondence should be addressed. Phone: 330-6722988. Fax: 330-6723816.
† Kyoto University.
‡ Kent State University.

(1) See, for example: Harvey, R. G. *Polycyclic aromatic hydrocarbons; Chemistry and carcinogenicity*; Cambridge Monographs on Cancer Research; Cambridge University Press: Cambridge, 1991. *Polycyclic Aromatic Hydrocarbons*; Harvey, R. G., Ed.; ACS Symposium Series 283; American Chemical Society: Washington, DC, 1985. Harvey, R. G. *Acc. Chem. Res.* **1981**, *14*, 218. Harvey, R. G..; Geacintov, N. E. *Acc. Chem. Res.* **1988**, *21*, 66. Harvey, R. G. In *The Handbook of Environmental Chemistry, Vol. 3, Part 1; PAHs and Related Compounds*; Neilson, A. H., Ed.; Springer-Verlag: Berlin, Heidelberg, 1998.

(2) Jerina, D. M.; Sayer, J. M.; Agrawal, S. K.; Yagi, H.; Levin, W.; Wood, A. W.; Conney, A. H.; Pruess-Schwartz, D.; Baird, W. M.; Pigott, M. A.; Dipple, A. In *Biological Reactive Intermediates, III*; Kocsis, J. J., Jollow, D. J., Witmer, C. M., Nelson, J. O., Snyder, R., Eds.; Plenum Publishing Corp.: New York, 1986.

10.1021/jo035133s CCC: $27.50
Published on Web 12/30/2003

examined by semiempirical (AM1, PM3) calculations,[5b] and molecular mechanics and dynamics were employed to probe the intercalation of BaP-triol-carbenium ion into model dinucleotides.[5c] Under stable ion conditions, BaP is protonated at C-6 in protic superacids.[6] The NMR data for the resulting carbocation were previously reported.[6] Upon two-electron oxidation with SbF_5/SO_2ClF, **1** gives a persistent 18π-electron dication with a 16π-electron periphery which sustains a paramagnetic ring current.[7] Neither GIAO (gauge independent atomic orbitals) NMR nor NICS (nucleus independent chemical shifts) (see computational protocol) was previously employed in theoretical studies of BaP and its metabolites. Therefore, the relative success of GIAO NMR as a tool for predicting NMR chemical shifts and charge delocalization patterns based on $\Delta\delta$ ^{13}C values in the BaP-derived carbocations and oxidation dications has remained unexplored.

Isomeric azulenophenalenes **2-4** (Figure 1) which formally result from fusing a phenalene moiety with azulene are the nonalternant isomers of **1**. Azuleno[5,6,7-*cd*]-phenalene **2** was synthesized by Jutz and associates[8] and was subsequently shown to be a strong carcinogen, comparable in metabolic activity to **1**.[9] Azuleno[1,2,3-*cd*]-phenalene **3** and azuleno[4,5,6-*cd*]phenalene **4** were later synthesized by Murata and co-workers.[10] Compound **3** is strongly mutagenic and weakly carcinogenic, whereas **4** is weakly mutagenic.[11]

Friedel−Crafts acylation and Vilsmeier formylation of **3** were reported to result in attack at C-1 and C-4.[12] Oxidation of **3** with *m*-CPBA gave 4-oxo-4*H*-benzo[*cd*]-fluoranthene **3A** and 1-oxo-1*H*-benzo[*cd*]fluoranthene **3B** (see Figure 1).[12] The regioselectivity of oxidation was explained by epoxidation at C-4/C-5 and at C-1/C-2, respectively, followed by ring opening to produce a delocalized tropylium cation which undergoes further nucleophilic attack by *m*-CPBA, followed by ring contraction and C−C bond cleavage, eventually leading to the observed products (see ref 12 for more mechanistic details on these steps).[12] The data suggest that electrophilic attack at C-1/C-4 sets the stage for subsequent nucleophile attachment onto the tropylium moiety.

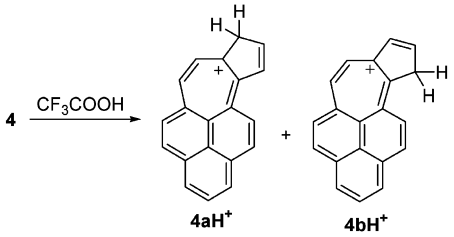

FIGURE 2. Protonation of **4** in trifluoroacetic acid.

Compound **4** is reversibly protonated in trifluoroacetic acid (TFA) (Figure 2) to give a mixture of **4aH**$^+$ (attack at C-8) and **4bH**$^+$ (attack at C-10) carbocations in 1:4 ratio (by NMR).[10b] Attack at C-10 relieves the nonbonded strain between H-10/H-11. The pronounced basicity of **4** was attributed to high thermodynamic stability of cyclohepta[*cd*]phenalenium structure.[10b]

No stable ion ^{13}C NMR data for azulenophenalenium ions are available. Given the prominent position of **1** in mechanistic carcinogenesis and its structural link to the nonalternant isomers **2**−**4**, a comparative theoretical study appeared timely.

In relation to our continuing interest in modeling biological electrophiles from PAHs[4b,13,14] and in the NMR characteristics and charge delocalization modes in the resulting carbocations[15] and oxidation dications,[16] and in connection to a recent theoretical study of carbocations and oxidation dications from azulene-PAHs,[17] we report here a DFT study on the carbocations and oxidation dications derived from **1** and its nonalternant analogues **2**−**4**.

Results and Discussion

Computational Protocols. Structures were optimized using molecular point groups shown in Table S1 (Supporting Information) by the density function theory (DFT) method at B3LYP/6-31G(d) level using the Gaussian 98 package.[18] Computed geometries were verified by frequency calculations. Furthermore, global minima were checked by manually changing initial geometries and by comparing the resulting optimized structures and their energies. NMR chemical shifts and NICS[19] values were calculated by the GIAO[20] method at the B3LYP/6-31G-

(3) Selected articles: Royer, R. E.; Lyle, T. A.; Moy, G. G.; Daub, G. H.; Vander Yagt, D. L. *J. Org. Chem.* **1979**, *44*, 3202. Lehr, R. E.; Taylor, C. W.; Kumar, S. *J. Org. Chem.* **1978**, *43*, 3462. Harvey, R. G.; Lee, H.-M.; Shyamasundar, N. *J. Org. Chem.* **1979**, *44*, 78. Gupta, S. C.; Islam, N. B.; Whalen, D. L.; Yagi, H.; Jerina, D. M. *J. Org. Chem.* **1987**, *52*, 3812. Islam, N. B.; Whalen, D. L.; Yagi, H.; Jerina, D. M. *J. Am. Chem. Soc.* **1987**, *109*, 2108. Yagi, H.; Sayer, J. M.; Thakker, D. R.; Levin, W.; Jerina, D. M. *J. Am. Chem. Soc.* **1987**, *109*, 838. Koreeda, M.; Gopalaswamy, R. *J. Am. Chem. Soc.* **1995**, *117*, 10595. Zajc, B. *J. Org. Chem.* **1999**, *64*, 1902. Lee, H.; Luna, E.; Hinz, M.; Stezowski, J. J.; Kiselyov, A. S.; Harvey, R. G. *J. Org. Chem.* **1995**, *60*, 5606.

(4) See, for example: (a) Melendez-Colon, V. J.; Luch, A.; Seidel, A.; Baird, W. M. *Chem. Res. Toxicol.* **2000**, *13*, 10. (b) Okazaki, T.; Laali, K. K.; Zajc, B.; Lakshman, M. K.; Kumar, S.; Baird, W. M.; Dashwood, W.-M. *Org. Biomol. Chem.* **2003**, *1*, 1509.

(5) (a) Lin, J.-H.; LeBreton, P. R.; Shipman, L. L. *J. Phys. Chem.* **1980**, *84*, 642. (b) Borosky, G. L. *J. Org. Chem.* **1999**, *64*, 7738. (c) Von Szentpaly, L.; Shamovsky, I. L. *Int. J. Quantum. Chem. Quantum Biology Symposium 22*, **1995**, 191. Von Szentpaly, L.; Shamovsky, I. *Mol. Pharmacol.* **1995**, *47*, 624.

(6) Laali, K. K.; Hansen, P. E.; Houser, J. J.; Zander, M. *J. Chem. Soc., Perkin Trans. 2*, **1995**, 1781. Laali, K. K. *Chem. Rev.* **1996**, *96*, 1873.

(7) Laali, K. K.; Tanaka, M.; Hansen, P. E. *J. Org. Chem.* **1998**, *63*, 8217.

(8) (a) Jutz, C.; Kirchlechner, R. *Angew. Chim., Int. Ed. Engl.* **1966**, *5*, 516. (b) Jutz, C.; Kirchlechner, R.; Seidel, H.-J. *Chem. Ber.* **1969**, *102*, 2301.

(9) (a) Buu-Hoi, N. P.; Hein, D. P.; Jutz, C.-H. *Naturwissenschaften* **1967**, *54*, 470. (b) Buu-Hoi, N. P.; Giao, N. B.; Jutz, C.-H. *Naturwissenschaften* **1970**, *57*, 499.

(10) (a) Murata, I.; Nakasuji, K.; Yamamoto, K.; Nakazawa, T.; Kayane, Y.; Kimura, A.; Hara, O. *Angew. Chem., Int. Ed. Engl.* **1975**, *14*, 170. (b) Naksuji, K.; Toda, E.; Murata, I. *Angew. Chem., Int. Ed. Engl.* **1977**, *16*, 784.

(11) Takahashi, Y.; Nagao, M.; Sugimura, T.; Todo, E.; Murata, I. *Mutat. Res.* **1980**, *78*, 295.

(12) Nakasuji, K.; Nakamura, T.; Murata, I. *Tetrahedron Lett.* **1978**, 1539.

(13) Laali, K. K.; Hansen, P. E. *J. Org. Chem.* **1997**, *62*, 5804. Laali, K. K.; Tanaka, M. *J. Org. Chem.* **1998**, *63*, 7280.

(14) Laali, K. K.; Okazaki, T.; Kumar, S.; Galembeck, S. E. *J. Org. Chem.* 2001, *66*, 780. Laali, K. K.; Okazaki, T.; Harvey, R. G. *J. Org. Chem.* **2001**, *66*, 3977. Laali, K. K.; Okazaki, T.; Hansen, P. E. *J. Org. Chem.* **2000**, *65*, 3816. Laali, K. K.; Okazaki, T.; Coombs M. M. *J. Org. Chem.* **2000**, *65*, 7399.

(15) Review: Laali, K. K.; Okazaki, T. *Annu. Rep. NMR Spectrosc.* **2002**, *47*, 149−214.

(16) Laali, K. K.; Okazaki, T.; Galembeck, S. E.; Siegel, J. S. *J. Org. Chem.* **2001**, *66*, 8701. Laali, K. K.; Tanaka, M. *J. Chem. Soc., Perkin Trans. 2*, **1998**, 2509. Laali, K. K.; Tanaka, M.; Fetzer, J. C. *J. Chem. Soc., Perkin Trans. 2* **1997**, 1315. Laali, K. K.; Hansen, P. E.; Gelerinter, E.; Houser, J. J. *J. Org. Chem.* **1993**, *58*, 4088.

(17) Okazaki, T.; Laali, K. K. *Org. Biomol. Chem.* **2003**, 3078.

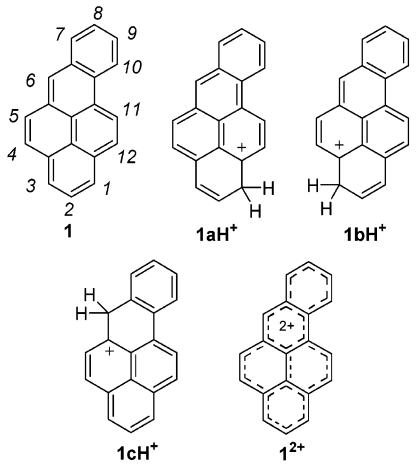

FIGURE 3. Benzo[*a*]pyrenes (**1**), protonated benzo[*a*]pyrenes (**1aH**$^+$−**1cH**$^+$), and the oxidation dication **1**$^{2+}$.

(d)//B3LYP/6-31G(d) level. NMR chemical shifts were referenced to TMS (GIAO magnetic shielding tensor = 183.7642 ppm; this value is related to the GIAO isotropic magnetic susceptibility for ^{13}C), calculated with a molecular symmetry of T_d at the same level of theory. For comparison, in selected cases, GIAO NMR chemical shifts were also computed at the B3LYP/6-311++G(d,p)//B3LYP/6-31G(d) level. NICS values were measured at the ring centroid (defined as simple average of Cartesian coordinates for all carbons in the ring). Table S1 (in Supporting Information) summarizes the total energies (*E*), zero-point energies (ZPE), and Gibbs free energies (*G*) for the neutral substrates, the carbocations, and the oxidation dications.

Benzo[*a*]pyrene (1). DFT-optimized structures of **1**, **1aH**$^+$, **1bH**$^+$, **1cH**$^+$, and **1**$^{2+}$ with C_s symmetry were calculated to be minima. In agreement with experiment,[6] the most stable arenium ion among various protonated benzo[*a*]pyrenes is **1cH**$^+$, which is protonated at the C-6 position. Other carbocations are more than 4 kcal/mol higher in energy (Figure 3 and Table S1, Supporting Information).

Optimized geometries for **1**, **1cH**$^+$, and the singlet **1**$^{2+}$ are shown in Figure S1 (Supporting Information) for comparison (the triplet dication was also found to be a minimum but considerably less stable that the singlet; see Table S1, Supporting Information). The largest changes in bond lengths in **1cH**$^+$ are for the C-5a/C-6 and C-6/C-6a bonds, which are noticeably longer due to rehybridization at C-6. A reasonable overall bond alternation scheme (shorter/longer relative to **1**) can be deduced for **1cH**$^+$. This feature is more pronounced in the dication **1**$^{2+}$. Figure S2 (Supporting Information) gives a summary of the experimental ^{13}C NMR data[6,7] for **1cH**$^+$ and **1**$^{2+}$ whereas the GIAO NMR data and NPA-derived charges (and changes in charges) for **1cH**$^+$ and **1**$^{2+}$ are gathered in Figure S3 (Supporting Information) for comparison. The NPA-derived sum of carbon and hydrogen charges are also shown.

The computed GIAO-^{13}C NMR data for **1cH**$^+$ and **1**$^{2+}$ are on average about 10 ppm lower than the experimental (superacid) ^{13}C chemical shifts. However, the correspondence based on the $\Delta\delta$ ^{13}C values is very good. For **1cH**$^+$, the largest changes in the chemical shifts are computed at C-5a and C-10b carbons. Large changes in both chemical shifts and the NPA-derived charges are observed within the pyreno moiety with limited charge delocalization into the benzo-ring. Positive charge in the dication **1**$^{2+}$is extensively delocalized throughout the periphery with C-6, C-1/C-3, C-7/C-9, and C-12 being distinctly more positive. These sites (especially C-6) are considered logical candidates for nucleophile attachment.

Figure 4a shows a plot of experimental ^{13}C values versus the GIAO shifts for **1cH**$^+$ and **1**$^{2+}$, illustrating very good overall linearity. Indeed, the computed δ ^{13}C values are well correlated with the experimental values by eq 1 (see below) with $R^2 = 0.9797$.

$$\delta\ ^{13}\mathrm{C(GIAO)} = 0.94\delta\ ^{13}\mathrm{C(exp)} - 3.57 \qquad (1)$$

The overall charge pattern deduced based on carbon charges, and the sum of carbon and hydrogen charges are similar. Correlations between the NPA-derived changes in the sum of charges over CH units versus GIAO-$\Delta\delta$ ^{13}C values and between the NPA-derived changes in carbon charges versus GIAO-$\Delta\delta$ ^{13}C are illustrated in Figures S4 and S5 (Supporting Information). These plots exhibit good linearity especially for the sum of CH charges.[21]

Overall, the GIAO-derived $\Delta\delta$ ^{13}C values and the NPA-derived changes in charges are in concert with experiment, demonstrating strong phenalenium ion character in**1cH**$^+$ and extensive charge delocalization throughout the periphery in **1**$^{2+}$. It is also interesting to note that the resulting charge pattern is the same as that for the benzylic carbocation formed via bay-region BaP-epoxide ring opening.[4b]

Sensitivity of the computed NMR chemical shifts to the size of the basis set is well documented.[22] In the context of the present study, and for comparison, the NMR chemical shifts for **1cH**$^+$ and **1**$^{2+}$ were also computed by the GIAO method at the augmented B3LYP/6-311++G(d,p)//B3LYP/6-31G(d) level. The experimental ^{13}C values are plotted against the GIAO shifts in Figure 4b. The computed δ ^{13}C values are correlated with the experi-

(18) Frisch, M. J.; Trucks, G. W.; Schlegel, H. B.; Scuseria, G. E.; Robb, M. A.; Cheeseman, J. R.; Zakrzewski, V. G.; Montgomery, J. A., Jr.; Stratmann, R. E.; Burant, J. C.; Dapprich, S.; Millam, J. M.; Daniels, A. D.; Kudin, K. N.; Strain, M. C.; Farkas, O.; Tomasi, J.; Barone, V.; Cossi, M.; Cammi, R.; Mennucci, B.; Pomelli, C.; Adamo, C.; Clifford, S.; Ochterski, J.; Petersson, G. A.; Ayala, P. Y.; Cui, Q.; Morokuma, K.; Malick, D. K.; Rabuck, A. D.; Raghavachari, K.; Foresman, J. B.; Cioslowski, J.; Ortiz, J. V.; Baboul, A. G.; Stefanov, B. B.; Liu, G.; Liashenko, A.; Piskorz, P.; Komaromi, I.; Gomperts, R.; Martin, R. L.; Fox, D. J.; Keith, T.; Al-Laham, M. A.; Peng, C. Y.; Nanayakkara, A.; Challacombe, M.; Gill, P. M. W.; Johnson, B.; Chen, W.; Wong, M. W.; Andres, J. L.; Gonzalez, C.; Head-Gordon, M.; Replogle, E. S.; Pople, J. A. Gaussian 98, Revision A.9, Gaussian, Inc., Pittsburgh, PA, 1998.

(19) Schleyer, P. v. R.; Maerker, C.; Dransfeld, A.; Jiao, H.; Hommes, N. J. v. E. *J. Am. Chem. Soc.* **1996**, *118*, 6317.

(20) Wolinski, K.; Hinton, J. F.; Pulay, P. *J. Am. Chem. Soc.* **1990**, *112*, 8251. Dichfield, R. *Mol. Phys.* **1974**, *27*, 789.

(21) It is important to realize that observation of a correlation between chemical shift and density (and charges) is by no means a general rule and it is not rare to find examples where such a relationship fails.

(22) For an authoritative review, see: Gauss, J. In *Modern Methods and Algorithms of Quantum Chemistry, Proceedings*, 2nd ed.; Grotendorst, J., Ed.; John von Neumann Institute for Computing: Julich, 2000; NIC Series, Vol. 3, pp 541−592 (http://www.fz-juelich.de/nic-series). For a recent illustrative example in carbocation chemistry. see: Siehl, H.-U.; Müller, T.; Gauss, J. *J. Phys. Org. Chem.* **2003**, *16*, 577.

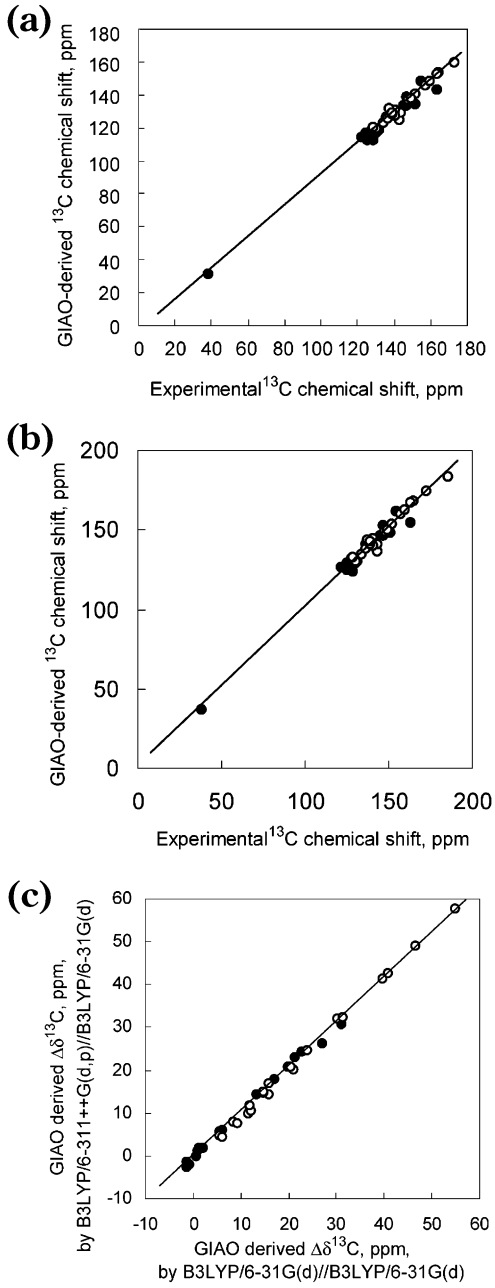

FIGURE 4. (a) Plot of experimental ^{13}C NMR chemical shifts versus GIAO-derived ^{13}C NMR chemical shifts for **1cH**$^+$ (●) and **1**$^{2+}$ (○). (b) Plot of experimental ^{13}C NMR chemical shifts versus GIAO-derived ^{13}C NMR chemical shifts at the B3LYP/6-311++G(d,p) level for **1cH**$^+$ (●) and **1**$^{2+}$ (○). (c) Plot of GIAO-derived $\Delta\delta$ ^{13}C NMR chemical shifts computed at the B3LYP/6-31G(d)//B3LYP/6-31G(d) level versus GIAO-derived $\Delta\delta$ ^{13}C NMR chemical shifts obtained at the B3LYP/6-311++G(d,p)//B3LYP/6-31G(d) level for **1cH**$^+$ (●) and **1**$^{2+}$ (○).

mental data by eq 2 (see below) with $R^2 = 0.977$ with a slope of near unity.

$$\text{GIAO-}\delta\ ^{13}\text{C} = 1.00 \exp \delta\ ^{13}\text{C} + 1.40 \qquad (2)$$

Figure 4c represents an overlay of experimental versus computed $\Delta\delta$ ^{13}C NMR values obtained at two different levels, showing that employing a larger basis set did not result in any significant changes in the correlation.

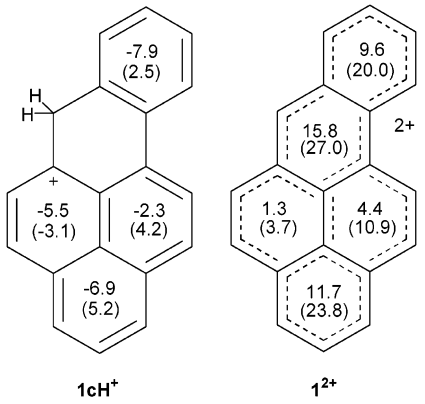

FIGURE 5. NICS for **1cH**$^+$ and **1**$^{2+}$ (ΔNICS values relative to those of **1** in parentheses).

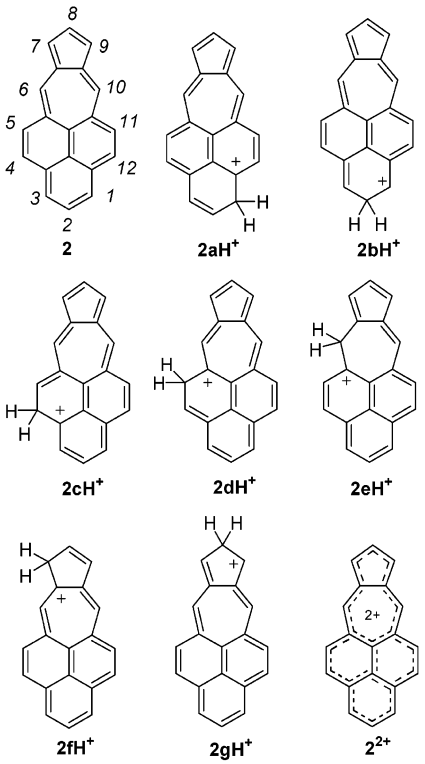

FIGURE 6. Azuleno[5,6,7-*cd*]phenalene (**2**), their protonated cations **2aH**$^+$−**2gH**$^+$, and oxidation dication **2**$^{2+}$.

Hence, we use the data computed at the B3LYP/6-31G-(d)//B3LYP/6-31G(d) level for further discussion.

Figure 5 summarizes the NICS and ΔNICS values. For **1cH**$^+$, the individual rings are still aromatic. For **1**$^{2+}$ there is a strong positive shift upon two-electron oxidation indicative of anti-aromaticity and consistent with the solution NMR-based data showing the presence of a paramagnetic ring current and paratropicity.[7]

Azuleno[5,6,7-*cd*]phenalene (2). As pointed out in the Introduction, compound **2** is a strong carcinogen comparable to BaP. The DFT-optimized structures of **2** with C_{2v} symmetry, **2fH**$^+$ (protonation at C-7) with C_s symmetry, and **2**$^{2+}$ with C_s symmetry (this geometry is almost the same as the C_{2v} symmetrical structure) were calculated to be global minima (see Figure 6 and Figure S6, Supporting Information). Whereas the singlet and

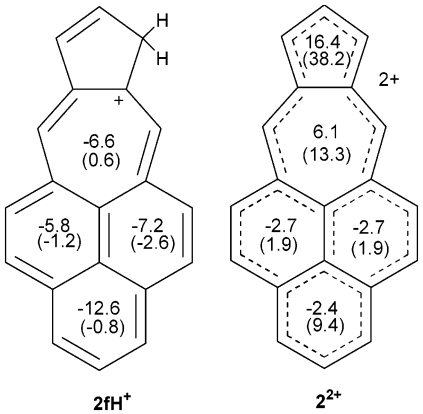

FIGURE 7. NICS for **2fH**$^+$ and **2**$^{2+}$ (ΔNICS values relative to those of **2** in parentheses).

triplet dications were both minima (C_s symmetry), the singlet dication was computed to be 20.1 kcal/mol more stable.

Among various possible carbocations that could be formed, protonation at C-7 (five-membered ring) clearly stands out as energetically most favored (Table S1, Supporting Information).

Optimized structures of **2**, **2fH**$^+$, and **2**$^{2+}$ and the computed bond lengths are shown in Figure S6 for comparison. The most noticeable bond-length changes in **2fH**$^+$ occur in the five-membered ring (protonation site) with several other bonds becoming shorter/longer in the phenalenium moiety. Changes in bond lengths are more pronounced in the dication.

The GIAO NMR and NPA-derived charges and their respective changes are illustrated in Figure S7 (Supporting Information). Positive charge in **2fH**$^+$ is extensively delocalized and the delocalization pattern represents fusion of a phenalenium moiety with an azulenium moiety. For the azulenium unit, the charge pattern is similar to that of parent azulenium ion,[17] except that C-12c does not carry positive charge.

The dication **2**$^{2+}$exhibits extensive charge delocalization throughout the periphery, with C-7/C-9 and C-1/C-3 identified as most susceptible for binding to nucleophiles.

It is noteworthy that a similar charge alternation pattern as that deduced for **2fH**$^+$ could be achieved in the carbocations resulting from epoxidation at the 7,8-bond, the 1,2-bond, or the 4,5-bond, followed by ring opening.

Based on NICS and ΔNICS (Figure 7), the phenalenium and tropylium moieties in **2fH**$^+$ are aromatic. The 18π-electron dication **2**$^{2+}$ with a 16π-periphery is at best borderline aromatic in the phenaleno moiety and antiaromatic in the azuleno moiety, with the five-membered ring exhibiting the largest positive NICS values.

Azuleno[1,2,3-*cd*]phenalene (3). Compound **3** is a strong mutagen and a weak carcinogen. Among various possible carbocations accessible by protonation, arenium ion of attack at C-1 (**3aH**$^+$) has the lowest energy followed by C-4 (**3cH**$^+$) which is 3.3 kcal/mol less stable (Figure 8 and Table S1, Supporting Information). These findings are in accord with the outcome of acylation and formylation of **3** mentioned in ref 12.

Optimized structures for **3**, **3aH**$^+$-**3dH**$^+$, **3gH**$^+$, and **3**$^{2+}$ with C_s symmetry and **3eH**$^+$, **3fH**$^+$, and **3hH**$^+$ with C_1 symmetry were calculated to be minima. The optimized geometries for **3** and **3**$^{2+}$ have almost C_{2v} symmetry. The computed structures for **3fH**$^+$ and **3hH**$^+$ with C_s symmetry were found to be transition states and less stable than a slightly distorted structure with C_1 symmetry (Figure 8; Figure S8 and Table S1, Supporting Information). The singlet and triplet dications of **3** are both minima, but the singlet is strongly favored

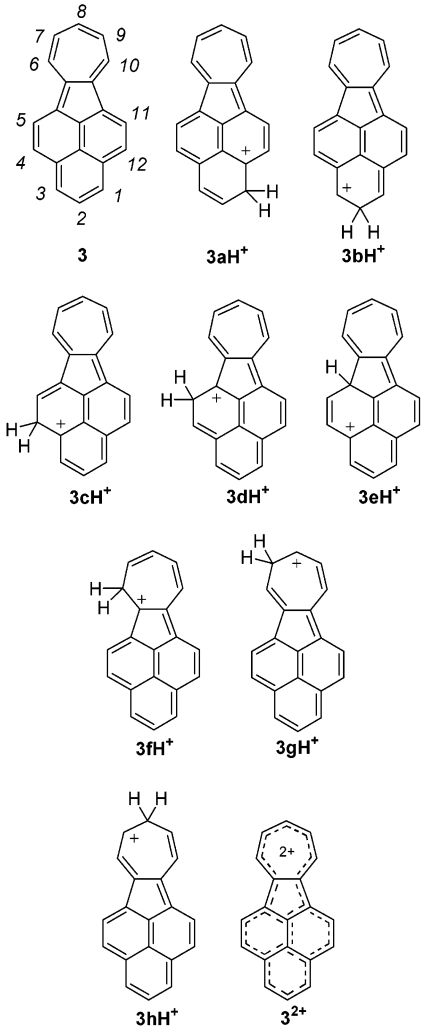

FIGURE 8. Azuleno[1,2,3-*cd*]phenalene (**3**), azuleno[1,2,3-*cd*]-phenalenium ions **3aH**$^+$−**3hH**$^+$, and the oxidation dication **3**$^{2+}$.

Optimized geometries and the bond-lengths for **3**, **3aH**$^+$ and **3**$^{2+}$ are collected in Figure S5 (Supporting Information). For **3aH**$^+$, the largest changes are at (and in the vicinity of) the ring undergoing attack and there is little bond variation in the tropylium unit. More pronounced bond-length variations are seen in **3**$^{2+}$.

The GIAO-derived ^{13}C shifts and the NPA-derived charges and their respective changes for **3aH**$^+$ and **3**$^{2+}$ are gathered in Figure S9 (Supporting Information).

Carbocation **3aH**$^+$ has a distinct tropylium ion character and is similar to Murata's proposed tropylium ion formed by *m*-CPBA epoxidation at the 4,5-positions.[12] This carbocation is clearly susceptible to nucleophilic attack at C-7/C-9 (based on changes in NPA charges attack at C-5/C-11 is also likely). Charge delocalization in the dication is more extensive with the largest $\Delta\delta$ ^{13}C values computed for C-1/C-3, C-4/C-12, and C-7/C-9.

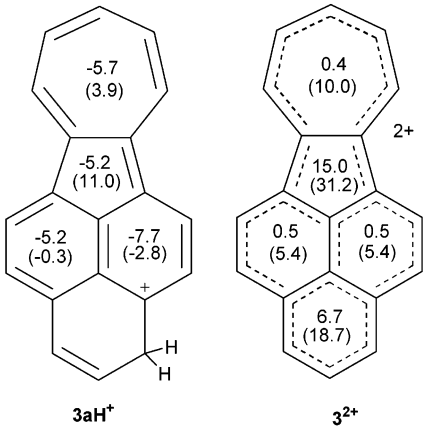

FIGURE 9. NICS for **3aH**$^+$ and **3**$^{2+}$ (ΔNICS values relative to those of **3** in parentheses).

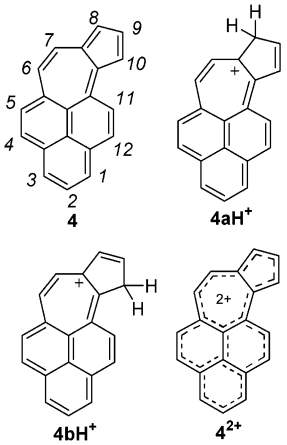

FIGURE 10. Azuleno[4,5,6-*cd*]phenalene (**4**), azuleno[4,5,6-*cd*]phenalenium ions **4aH**$^+$ and **4bH**$^+$, and the oxidation dications **4**$^{2+}$.

Computed NICS and ΔNICS values (Figure 9) show small positive shifts in the individual rings for **3aH**$^+$ indicating that the system is still aromatic. The large positive shifts observed in **3**$^{2+}$ especially in the five-membered ring are indicative of anti-aromaticity of the singlet dication.

Azuleno[4,5,6-*cd*]phenalene (4). This compound is weakly mutagenic (less active than **2** and **3**). All possible protonations sites (twelve carbocations) were calculated, among them there was a clear preference for **4aH**$^+$(attack at C-8) and **4bH**$^+$ (attack at C-10) (Table S1, Supporting Information, and Figure 10) with **4bH**$^+$ being 0.7 kcal/mol lower in energy than **4aH**$^+$. The computed relative stabilities match closely Murata's previously reported 1:4 ratio for **4aH**$^+$ and **4bH**$^+$ formed in TFA.[10b]

The optimized structures for **4**, **4bH**$^+$, and **4**$^{2+}$ with C_s symmetry were calculated to be minima, whereas the computed structure for **4aH**$^+$ with C_s symmetry was found to be a transition state and less stable than a slightly bent structure with C_1 symmetry.

The optimized geometries with computed bond lengths for neutral **4**, **4aH**$^+$, **4bH**$^+$ as well as singlet and triplet **4**$^{2+}$ are collected in Figure S10 (Supporting Information). For the carbocations, the largest variations in bond-lengths are seen in the azuleno moiety (the five-membered ring in particular), whereas for the dications, changes in bond-lengths are more extended and involve almost the entire system.

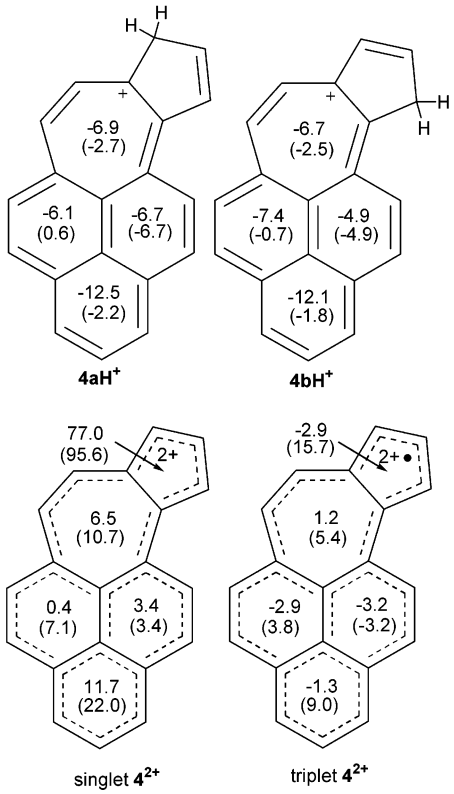

FIGURE 11. NICS for **4aH**$^+$, **4bH**$^+$, and for singlet and triplet **4**$^{2+}$ (ΔNICS values relative to those of **4** in parentheses).

Figure S11 (Supporting Information) gives a summary of the GIAO-^{13}C shifts and the NPA-derived charges and their respective changes for **4aH**$^+$ and **4bH**$^+$ carbocations. Contrary to the carbocations derived from **3** and **2**, charge delocalization in **4aH**$^+$ and **4bH**$^+$ is limited to a cyclopentenyl cation and a conjugated carbon in the seven-membered ring with additional minor delocalization into the phenaleno unit. Interestingly, for hydrocarbon **4**, the triplet dication lies 5.1 kcal/mol lower in energy than the singlet dication (Table S1, Supporting Information). GIAO NMR shifts and the NPA-derived charges for the singlet and triplet dications and their respective changes are summarized in Figure S12 (Supporting Information) for comparison.

A striking feature in both singlet and triplet dication is localization of positive charge in the five-membered ring as well as on C-6 with additional (less pronounced) delocalization into the phenaleno moiety. There are only minor differences in the overall charge delocalization patterns in the singlet and triplet dications.

NICS and ΔNICS values (Figure 11) suggest that the individual rings in **4aH**$^+$ and **4bH**$^+$ undergo slight positive shifts and remain aromatic. The singlet dication, on the other hand, exhibits an unusually large positive shift in the five-membered ring.[23] This feature is no longer observed in the energetically more favorable triplet dication.

(23) For other examples of unusually high NICS values, see ref 17 and comments therein.

Comparative Discussion and Summary

The following key points concerning carbocation and dication formation from benzo[*a*]pyrene emerge from DFT calculations and tie in with the available experimental data: (i) electrophilic attack occurs at C-6 forming a highly delocalized arenium ion with strong phenalenium ion character in which individual rings are aromatic, and with limited delocalization into the benzo ring; (ii) good correlation exists between the experimental NMR data in superacid media and GIAO NMR; (iii) presence of reasonable correlations between the NPA-derived charges and GIAO chemical shifts; (iv) NICS data for the dications are consistent with the experimentally observed paratropicity in the dication; (v) the established charge delocalization path in BaP carbocation is the same as that via the "benzylic" carbocation formed by bay-region BaP epoxide ring opening; (vi) the most likely sites for nucleophilic attack on the carbocation and oxidation dication have been singled out. The combined information is useful toward designing experiments that would model adduct formation between the BaP "benzylic" carbocation and biologically relevant nucleophiles.

Electrophilic attack on azulenophenalene **2** occurs at C-7. The resulting carbocation is highly delocalized and has the characteristics arising from fusing of an azulenium moiety with a phenalenium moiety. The tropylium/phenalenium moieties are aromatic. Whereas positive charge in the singlet $\mathbf{2}^{2+}$ is extensively delocalized throughout the periphery, the C-7/C-9 and C-1/C-3 are most positive. The dication is anti-aromatic in the azuleno and borderline-aromatic in the phenaleno moieties.

The most favored site for electrophilic attack on azulenophenalene **3** is C-1 followed by C-4. The carbocation remains aromatic. Charge delocalization mapping in the arenium ion is indicative of strong tropylium character with lesser degree of phenalenium character. Subsequent nucleophilic attack on the tropylium moiety (at C-7/C-9) is a logical next step and could well be the pathway that leads to binding to nucleotide. Positive charge in the singlet $\mathbf{3}^{2+}$ is extensively delocalized but C-1/C-3 and C-7/C-9 (at the two ends of the molecule) are most positive and represent logical sites for attack by nucleophile. As with $\mathbf{1}^{2+}$, the dication derived from **3** is antiaromatic and should be paratropic.

The most favored sites for electrophilic attack on azulenophenalene **4** are C-10 and C-8. The resulting carbocations exhibit limited charge delocalization paths (mainly confined to the 5-membered ring). Individual rings in the arenium ions are aromatic. Unlike other isomeric azulenophenalenes, the triplet dication here is more stable than the singlet dication. Positive charge in the singlet and triplet dications are delocalized throughout the system, but the five-membered ring is most positive. The singlet dication is strongly antiaromatic whereas the more stable triplet is at best borderline-aromatic.

In conclusion, the present DFT study extends the available stable ion data on BaP carbocations and dications and provides the first glance into the electrophilic chemistry of its nonalternant analogues for which limited chemical and biological data and no stable ion data are so far available.

Acknowledgment. We are grateful to the reviewers for helpful suggestions and comments. This work was supported in part by the NCI of NIH (R15 CA78235) and by a Grant-in-Aid for Young Scientists (B) 15710160 from the Japan Society for the Promotion of Science (JSPS).

Supporting Information Available: Table S1: Electronic energies, zero point energies, and Gibbs free energies obtained from DFT calculations for the studied molecules and cations at the B3LYP/6-31G(d) level. Tables S2−S15 and Figures S1, S6, S8, and S10: Cartesian coordinates and optimized structures for **1**, $\mathbf{1cH}^{+}$, $\mathbf{1}^{2+}$, **2**, $\mathbf{2fH}^{+}$, $\mathbf{2}^{2+}$, **3**, $\mathbf{3aH}^{+}$, $\mathbf{3}^{2+}$, **4**, $\mathbf{4aH}^{+}$, $\mathbf{4bH}^{+}$, and $\mathbf{4}^{2+}$. Figure S2: Experimental ^{13}C NMR chemical shifts for $\mathbf{1cH}^{+}$ and $\mathbf{1}^{2+}$. Figures S3, S7, S9, S11, and S12: Computed ^{13}C NMR chemical shifts and NPA-derived charges for $\mathbf{1cH}^{+}$, $\mathbf{1}^{2+}$, $\mathbf{2fH}^{+}$, $\mathbf{2}^{2+}$, $\mathbf{3aH}^{+}$, $\mathbf{3}^{2+}$, $\mathbf{4aH}^{+}$, $\mathbf{4bH}^{+}$, and $\mathbf{4}^{2+}$. Figures S4 and S5: Correlation between the NPA-derived changes in the sum of charges over CH units and GIAO-derived $\Delta\delta$ ^{13}C and correlation between the change in NPA-derived carbon charges and GIAO-derived $\Delta\delta$ ^{13}C for $\mathbf{1cH}^{+}$ and $\mathbf{1}^{2+}$. This material is available free of charge via the Internet at http://pubs.acs.org.

JO035133S